

Optical cloaking using alternate Raman gain and free-space media in the presence of spatially distributed pump fields

Chengjie Zhu,^{1,2} L. Deng,² E. W. Hagley,² and Mo-Lin Ge³

¹East China Normal University, Shanghai 200062, China

²National Institute of Standards & Technology, Gaithersburg, Maryland 20899, USA

³Theoretical Physics Division, Chern Institute of Mathematics, NanKai University, Tianjin 300071, China

(Received 24 July 2013; published 22 October 2013)

We discuss an optical “cloaking” scheme using three-level active Raman gain media in tandem in the presence of a spatially distributed pump field. Using eikonal approximation we first derive analytically the deflection angle and show that the trajectory of light can be controlled dynamically using a spatially distributed pump. We further show an excellent agreement of analytical results with a full numerical calculation of the Maxwell equation for the probe field propagating across regions where an object is embedded. Our results show that the probe light travels around the object under detection, achieving the desired spatial cloaking of the object.

DOI: [10.1103/PhysRevA.88.045804](https://doi.org/10.1103/PhysRevA.88.045804)

PACS number(s): 42.65.Dr, 42.50.Gy

Introduction. In the field of optics, “cloaking” refers to the phenomenon in which a light wave passes through an object without being disturbed and affected either due to spatial light beam propagation manipulation (by the surface or structure composition of the object) or due to certain types of active interference effects. For instance, artificial materials referred to as metamaterials can bend a light wave around an object [1] without actually distorting the wave front so as to leave a detectable effect. Many theoretical and experimental works about optical cloaking have been reported to date by using metamaterials [2–4]. In all proposals for invisibility, the physical mechanism of the invisibility or cloaking is the manipulation of optical parameters (such as permittivity and permeability) by engineering the structures of the metamaterials so that a light wave of a specific wavelength is guided around the region of interest and later reverted back to its original direction of propagation.

While metamaterials and engineered structures with their exotic artificial properties are the most promising candidates for realization of object invisibility, it is widely known that room temperature atomic media can also exhibit similar light wave bending and guiding effects [5]. Schlessler [6] first observed the deflection of a light beam at the interface of a glass window and Cs vapor due to a transverse-magnetic field. Many experimental studies [7–11] and theoretical investigations [12–16] have led to the understanding of dynamic light beam deflection in the presence of external fields. Recently, experimental observation of light ray bending in electromagnetically induced transparency (EIT) medium using an inhomogeneous magnetic field [10] and spatially distributed light control field [11] have been reported and also subsequently studied theoretically.

In this work we describe a different approach to realize optical cloaking using an atomic medium driven by an inhomogeneous pump field. The key differences of our work in comparison with results available in literature are: (1) the use of a Raman gain medium rather than a lossy EIT medium; (2) large light wave bending and guiding effect than EIT scheme and the elimination of significant loss associated with the EIT scheme, and (3) the complete object or target evading propagation demonstrated both with classical eikonal

approximation and full numerical simulation. These features provide a clear conclusion that an active Raman gain medium is a superior scheme in light ray guiding in atomic media.

Theoretical Model. We consider a system that consists of three cells filled with rubidium atomic gas with length L_0 , $2L_0$, and L_0 , respectively. Each cell is separated by a vacuum component with the same length L_1 . A far-off-resonant pump field with a spatially inhomogeneous distribution couples the transition between the ground state and the excited state with a large one-photon detuning to avoid spontaneous emissions. A probe field with a Gaussian profile drives the transition between the excited state and a metastable state. A typical three-level ARG configuration is formed if the initial population are in the ground state [see Fig. 1(b)].

The basic principle of operation described here is that the propagation path of the probe field is alternatively changed by the pump field in different segments of the medium so that the probe field first clears the object under detection and later resumes its original propagation direction.

The medium under consideration consists of a lifetime broadened three-state atomic system where the energy of state $|j\rangle$ is $\hbar\omega_j$ [Fig. 1(b)]. A strong and spatially distributed pump field of angular frequency ω_L couples the upper electronic state $|1\rangle$ to a fully occupied ground state $|0\rangle$ with a large one-photon detuning $\delta_1 = \omega_L - (\omega_1 - \omega_0)$. A weak probe field of angular frequency ω_p couples state $|1\rangle$ to state $|2\rangle$ with a two-photon detuning $\delta_2 = \omega_L - \omega_p - (\omega_2 - \omega_0)$. In this three-level ARG system [17,18], $2\Omega_L$ and $2\Omega_p$ are the Rabi frequencies of the coupling and probe fields, respectively. Under electric-dipole and rotating-wave approximations, we obtain the Hamiltonian in the interaction picture

$$\hat{H}_I = -\hbar \left[\sum_{i=1}^2 \delta_i |i\rangle\langle i| + \Omega_L |1\rangle\langle 0| + \Omega_p |1\rangle\langle 2| + \text{H.c.} \right], \quad (1)$$

which leads to the equations of motion for atomic response, i.e.,

$$\left(i \frac{\partial}{\partial t} + d_2 \right) A_2 + \Omega_p^* A_3 = 0, \quad (2a)$$

$$\left(i \frac{\partial}{\partial t} + d_3 \right) A_3 + \Omega_L A_1 + \Omega_p A_2 = 0. \quad (2b)$$

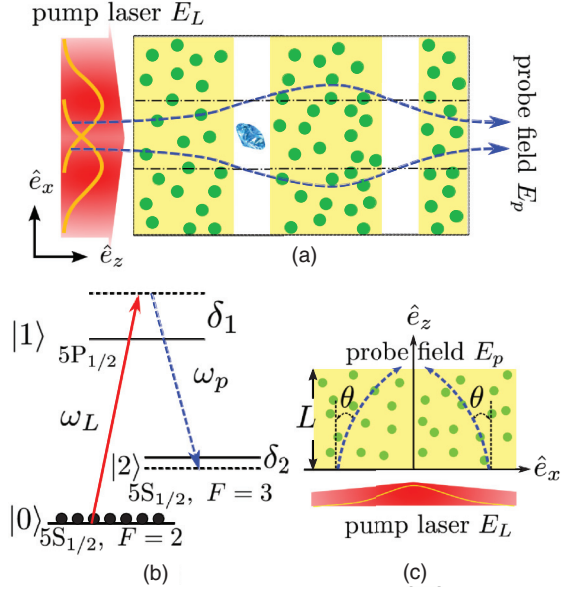


FIG. 1. (Color online) (a) Optical cloaking in active Raman gain medium under a spatially distributed pump field. (b) Three-level active Raman gain scheme with laser coupling. (c) Probe light deflection in the active Raman gain medium under a strong pump field with a Gaussian-type spatial distribution.

Here A_j ($j = 0$ to 2) is the probability amplitude of the bare atomic state $|j\rangle$ (with angular frequency ω_j) and $d_j = \delta_j + i\gamma_j$ with γ_j being the atomic decay rate of the state $|j\rangle$ ($j = 1, 2$). The normalized condition $\sum_{j=1}^3 |A_j|^2 = 1$ is understood for a closed system. In order to suppress a large optical pumping and a significant temperature-related Doppler effect, we assume that the one-photon detuning is much larger than the other parameters of the system, i.e., $|\delta_1|$ is much larger than the Rabi frequencies, Doppler broadened linewidths, atomic coherence decay rates, and frequency shift induced by the coupling laser field. In Fig. 1 we have assumed, for simplicity, a copropagation beam geometry, although it can be shown that the similar effect also occurs with the pump and probe propagating perpendicular to each other [19].

In the linear regime, the probability amplitude of the atomic state can be worked out by using multiorder adiabatic theory. Taking $A_i = A_i^{(0)} + \lambda A_i^{(1)}$ ($i = 0, 1, 2$), where λ is a small parameter characterizing the interaction order and letting, for a weak probe field, $\Omega_p = \lambda \Omega_p^{(1)}$ we obtain the zeroth order adiabatic solutions of Eqs. (2), i.e., $A_0^{(0)} = 1/\sqrt{1 + |\Omega_L/d_1|^2}$, $A_1^{(0)} = -\Omega_L/(d_1\sqrt{1 + |\Omega_L/d_1|^2})$, and $A_2^{(0)} = 0$. The first order adiabatic solutions of the probability amplitude of the atomic states can thus be obtained by solving Eqs. (2) iteratively, yielding the linear probe-field susceptibility

$$\chi_p^{\text{ARG}} = \frac{\mathcal{N}_a |\mathbf{p}_{21}|^2}{\varepsilon_0 \hbar \Omega_p} A_1^{(0)} A_2^{*(1)} = -\frac{\mathcal{N}_a |\mathbf{p}_{21}|^2}{\varepsilon_0 \hbar} \frac{|\Omega_L|^2}{(\delta_2 - i\gamma_2)(|d_1|^2 + |\Omega_L|^2)}, \quad (3)$$

where \mathcal{N}_a is the atomic density and \mathbf{p}_{21} is the dipole momentum on the transition $|1\rangle \leftrightarrow |2\rangle$.

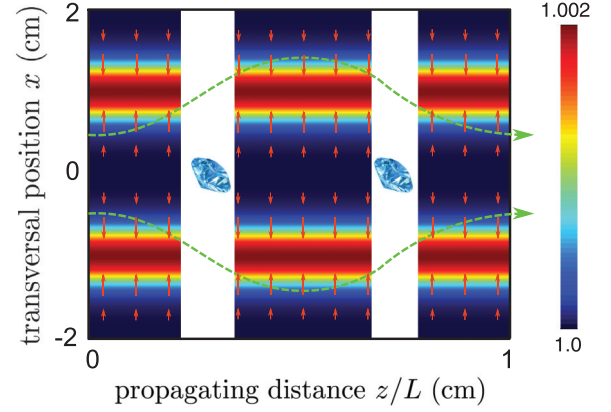


FIG. 2. (Color online) The refractive index of the probe field as functions of the transversal position x and the propagating distance z . The vector arrows indicate the bending direction and the magnitude of the deflection angle. The one- and two-photon detunings are $\delta_1 = 2$ GHz and $\delta_2 = -800$ kHz, respectively, and the pump field Rabi frequency is $\Omega_L^{(0)} = 100$ MHz. Other system parameters are given in the text.

The index of refraction for probe field is defined as

$$n = \sqrt{1 + \chi_p^{\text{ARG}}} \approx 1 + \frac{1}{2} \chi_p^{\text{ARG}}, \quad (4)$$

if $\chi_p^{\text{ARG}} \ll 1$. Generally, the refractive index n can be decomposed as $n = n' + in''$, where n' and n'' are the real and imaginary parts of the refractive index. Clearly both n' and n'' become space dependent if the pump laser Ω_L has spatial inhomogeneity. This leads to a deflection of the probe field with spatially dependent gain.

In our model we assume that the pump field has a spatially inhomogeneous distribution which is given by

$$\Omega_L(x) = \Omega_L^{(0)} [e^{-(x-1)^2/\sigma_L^2} + e^{-(x+1)^2/\sigma_L^2}], \quad (5)$$

where $\Omega_L^{(0)}$ is the peak value of the pump laser and σ_L is the $1/e$ radius of a single Gaussian profile. The refractive index is then given by

$$n'(x) \approx 1 - \frac{\mathcal{N}_a |\mathbf{p}_{21}|^2}{2\varepsilon_0 \hbar |d_1|^2} \times \frac{|\Omega_L^{(0)}|^2 \delta_2}{(\delta_2^2 + \gamma_2^2)} [e^{-2(x-1)^2/\sigma_L^2} + e^{-2(x+1)^2/\sigma_L^2}], \quad (6)$$

which leads to the deflection of the probe field for its spatial inhomogeneity. By using the eikonal approximation [20], the deflection angle of the probe field is given by

$$\theta \approx L \nabla_x (n')|_{x=x_0} \quad (7)$$

for a small deflection angle [21].

In Fig. 2 we plot the refractive index $n'(x)$ as a function of the spatial coordinate x . The parameters we used in our calculation are typical of those reported in literature. Specifically, we consider a rubidium gas cell with atomic density $1 \times 10^{12} \text{ cm}^{-3}$, $\gamma_2 = 10$ kHz, $\gamma_1 = 600$ MHz, $\mathbf{p}_{01} = \mathbf{p}_{21} = 3.5 \times 10^{-29} \text{ C m}$, $\delta_1 = 2$ GHz, and $\delta_2 = -800$ kHz for ARG configuration. The transversal width of the Gaussian profile is $\sigma_L = 0.5$ cm and the total length of the system is about $L = 35$ cm with $L_0 = 7.5$ and $L_1 = 2.5$, respectively.

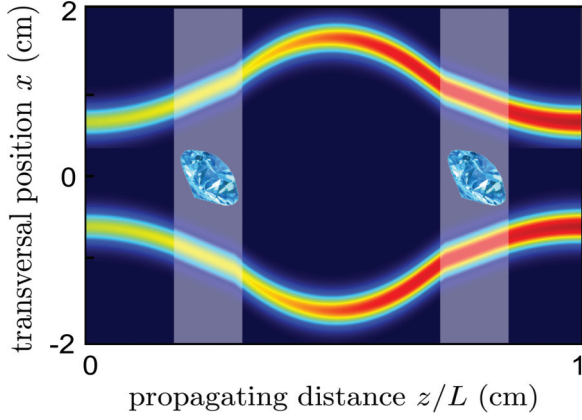


FIG. 3. (Color online) Numerical simulation of the beam propagation in ARG media. The initial probe field is $\Omega_p = \Omega_p^{(0)} \exp[-(x - x_0)^2/\sigma_p^2]$, where $\sigma_p = 0.15$ cm is the linewidth of the probe field. The incident position is chosen as $x_0 = \pm 0.6$ cm. The one- and two-photon detunings are $\delta_1 = 2$ GHz and $\delta_2 = -800$ kHz, respectively, and the pump field Rabi frequency is $\Omega_L^{(0)} = 100$ MHz. Other system parameters are given in the text.

With our parameters the refractive index changes greatly as the transversal position varies, which leads to a significant light deflection along the transversal axis. The direction and the strength of the deflection is demonstrated by the vector arrow as shown in Fig. 2. Utilizing this spacial distribution of the refractive index, we can realize the optical cloaking in this system. Provided that a probe field enters into the first cell, the trajectory of the probe field bends to avoid the target in the following vacuum regime. When it enters into the second cell, the probe field bends to the opposite side due to the change of the change of the gradient of the refractive index. Then it crosses over another vacuum regime and enters into the third cell to adjust its propagating direction along the z axis. Therefore, it is possible to control the trajectory of the probe field dynamically and achieve the optical cloaking in our model.

We have carried out numerical calculations to validate the above conclusions obtained by eikonal approximation. We first cast the Helmholtz equation for our system as

$$\nabla^2 E + 2\nabla[E \cdot \nabla(\ln n)] + \frac{\omega_p^2}{c^2} n^2 E = 0, \quad (8)$$

where n is the refractive index which can be expressed as $n(x) = n_0 + \delta n(x)$ with $n_0 = 1$. Under the slow varying amplitude approximation and paraxial approximation [22], Eq. (8) can be written as

$$i \frac{\partial E_p}{\partial z} = \frac{1}{2n_0 k_p} \left(\frac{\partial^2 \delta n}{\partial x^2} E_p + 2 \frac{\partial \delta n}{\partial x} \frac{\partial E_p}{\partial x} + \delta n \frac{\partial^2 E_p}{\partial x^2} \right) - \frac{1}{2k_p} \frac{\partial^2 E_p}{\partial x^2} - \frac{k_p \delta n}{n_0} E_p. \quad (9)$$

We numerical integrate Eq. (9) using a Gaussian-type initial probe field injected at various locations, i.e., $\Omega_p = \Omega_p^{(0)} \exp[-(x - x_0)^2/\sigma_p^2]$, where the beamwidth is characterized by $\sigma_p = 0.15$ cm. The incident position is chosen as $x_0 = \pm 0.6$ cm.

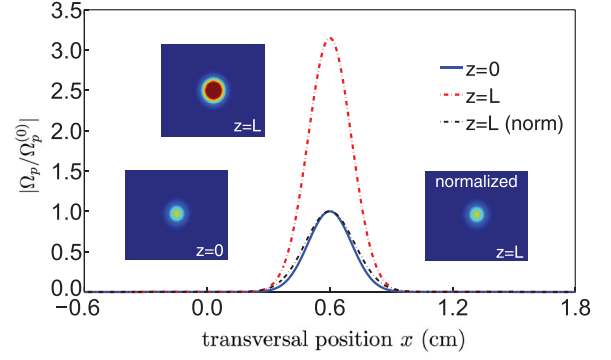


FIG. 4. (Color online) Plot of FWHMs of the transverse beam distribution at the entrance (blue curve) and at the exit (red dashed curve). The intensity normalized beam transverse distribution (black dash-dotted curve) shows negligible beam distortion.

In Fig. 3 we show the numerical simulation of Eq. (9) by using the initial condition given above and parameters used in generating Fig. 2. It is seen that the probe field first cleared the object under detection by the ARG medium in the first vapor cell. Its propagation direction is reverted in the second Raman gain medium and later the original direction of probe propagation is recovered by the beam manipulation in the third Raman gain medium. These results agree well with the prediction based on the classical eikonal approximation. Due to the gain nature of the media used the probe field is amplified during the operation. We note that it is straightforward to add an absorption layer or an electromagnetically induced-transparency (EIT) medium near the exit. This provides adjusted attenuation of the amplified probe field that renders the exit beam indistinguishable from the input beam, and thereby achieves the purpose of spacial cloaking of the object under detection. Such post-propagation reshaping remedies, however, cannot be easily applied to any solely EIT-based scheme where probe field spatial distortions are often severe in the middle interaction region due to the group velocity distribution. This shows the superior performance of the coherent amplification scheme we treated here. In Fig. 4 we show the full-width half-maximum (FWHM) of the probe beam transverse distribution which exhibits very little beam distortion.

In conclusion, we have presented a different approach to realize the optical cloaking using alternating Raman gain and free-space (possibly absorption) media. The probe light beam experiences propagation trajectory changes in various Raman gain media due to a spatially distributed pump field, resulting in probe beam bending and therefore avoided detection of the object. This approach is fundamentally different from the propagation interference effect produced by metamaterials with very different and large quasistatic permittivity and permeability in absence of the external fields. In the atomic medium, these quantities are unchanged in the absence of the external field and it is the dynamic general susceptibility of the system in the external fields that gives rise to the light bending effects.

Acknowledgments. C.J.Z. acknowledge the supported by NSF-China under Grants No. 10874043 and No. 11174080, and by the Chinese Education Ministry Reward for Excellent Doctors in Academics under Grant No. MXRZZ2010007.

- [1] J. B. Pendry, D. Schurig, and D. R. Smith, *Science* **312**, 1780 (2006).
- [2] W. Cai, U. K. Chettiar, A. V. Kildishev, and V. M. Shalaev, *Nat. Photon.* **1**, 224 (2007).
- [3] T. Ergin, N. Stenger, P. Brenner, J. B. Pendry, and M. Wegener, *Science* **328**, 337 (2010).
- [4] X. Chen, Y. Luo, J. Zhang, K. Jiang, J. B. Pendry, and S. Zhang, *Nat. Commun.* **2**, 176 (2011).
- [5] M. Born and E. Wolf, *Principles of Optics*, 7th (expanded) ed. (Cambridge University Press, Cambridge, UK, 1999).
- [6] R. Schlessler and A. Weis, *Opt. Lett.* **17**, 1015 (1992).
- [7] R. Holzner *et al.*, *Phys. Rev. Lett.* **78**, 3451 (1997).
- [8] G. T. Purves, G. Jundt, C. S. Adams, and I. G. Hughes, *Eur. Phys. J. D* **29**, 433 (2004).
- [9] R. R. Moseley, S. Shepherd, D. J. Fulton, B. D. Sinclair, and M. H. Dunn, *Phys. Rev. Lett.* **74**, 670 (1995).
- [10] L. Karpa and M. Weitz, *Nat. Phys.* **2**, 332 (2006).
- [11] V. A. Sautenkov, H. Li, Y. V. Rostovtsev, and M. O. Scully, *Phys. Rev. A* **81**, 063824 (2010).
- [12] M. D. Lukin, *Rev. Mod. Phys.* **75**, 457 (2003).
- [13] D. L. Zhou, L. Zhou, R. Q. Wang, S. Yi, and C. P. Sun, *Phys. Rev. A* **76**, 055801 (2007).
- [14] Q. Sun, Y. V. Rostovtsev, and M. S. Zubairy, *Phys. Rev. A* **74**, 033819 (2006).
- [15] C. J. Zhu, L. Deng, and E. W. Hagley, *Phys. Rev. A* **88**, 013841 (2013).
- [16] C. J. Zhu, L. Deng, and E. W. Hagley, *Opt. Lett.* **38**, 2363 (2013).
- [17] L. Deng and M. G. Payne, *Phys. Rev. Lett.* **98**, 253902 (2007).
- [18] C. J. Zhu, C. Hang, and G. X. Huang, *Eur. Phys. J. D* **56**, 231 (2010).
- [19] The main difference is the residual two-photon Doppler shift between the two beams.
- [20] K. V. Shajesh, *Eikonal Approximation*, Department of Physics and Astronomy, University of Oklahoma, USA.
- [21] Here we have assume that the gradient of the linear susceptibility is approximately the same as that at the incident point x_0 , which is valid for small deflection.
- [22] Propagation correction beyond paraxial approximation becomes important when the angle of deviation exceeds 0.2 rad, see L. Zhang, T. N. Dey, and J. Evers, *Phys. Rev. A* **87**, 043842 (2013). However, even in such cases, paraxial approximation is still a good first step since the corrections to the tails of transverse profile often play minor role in the process, especially when a filter or absorption layer is included at the exit of the system we treated.